Numerical Simulation and Parametric Study of Forced Convective Condensation in Vertical Channel

R. K. Kamali [i], A. Abbassi [ii] *, S. A. Sadough Vanini [iii] and M. Saffar Avval[iv]

Received 02 March 2008; received in revised 03 August 2008; accepted 12 January 2009

ABSTRACT

Forced convective condensation in vertical channel is investigated numerically. The condensation boundary layers that occur due to temperature difference between the walls and saturation temperature of steam is simulated by the volume of fluid (VOF) method. The effect of variations in the hydraulic diameter, steam velocity, Re number and temperature difference between the wall and saturation temperature of inlet steam on heat transfer coefficients are investigated. Simulation results showed that the condensation length and heat transfer coefficient increase by the increase in the amount of inlet velocity and Reynolds number of inlet steam. Also, it was seen a reduction in temperature difference between the wall and saturated steam.

KEYWORDS

Condensation, Numerical simulation, Vertical channel, Heat transfer coefficient.

1. INTRODUCTION

There is a huge competition between different types of heat exchangers. Because of high amount of material cost, it is very important task to design heat exchangers more compact in order to decrease the material consumption. It seems that using of the plate type heat exchangers is extremely grown up in industry. Using the plate type heat exchangers instead of shell and tube type significantly decrease the volume of the system and make the system compact and portable. As the pressure drop during the condensation and evaporation phenomena is usually high so design of the plate type heat exchangers for producing distilled water from saturated steam with minimum amount of the pressure drop is very complicated task [1,2]. Some experimental and theoretical works have been done by some researchers [3-14] in order to define heat transfer coefficients and pressure drop between the plates. Most flow regime studies on two-phase flow were performed in large hydraulic diameter. The distinctive feature of two phase flow in plate type heat exchangers with small gap between the plates is that the surface tension may play a significant role in flow pattern transitions.

Recently some new researches have been done based on two phase flow phenomena in multiple effect desalination systems with shell and tube and plate type heat exchangers [15-17]. It is very interesting subject to do research on the possibility of substituting the plate type heat exchangers instead of shell and tube type in multiple effect desalination. Since in plate type condensers in these systems, there is forced convective condensation between the plates.

This paper is dealt with a numerical model to simulate laminar and turbulent steam condensation between parallel plates by volume of fluids method (VOF). The interface mass transfer due to condensation will be considered as a source term in the energy equation. In order to define mass and energy source terms in equations, some UDF's were developed and coupled with Fluent software. The effects of vapor inlet velocity, wall temperature, and hydraulic diameter on condensation will also be investigated. This simulation helps the designers to obtain heat transfer coefficient of condensation flow, required heat transfer surface area and required number of plates in plate type condensers.

2. PHYSICAL MODEL

The geometrical configuration and physical model of condensation in vertical channel is shown in Figs.1 and 2.

i R. K. Kamali is with the Department of Mechanical Engineering, Amirkabir University of Technology, Tehran, Iran (E-mail: kouhikamali@aut.ac.ir)
ii * Corresponding Author, A. Abbassi is with the Department of Mechanical Engineering, Amirkabir University of Technology, Tehran, Iran (E-mail: abbassi@aut.ac.ir)
iii S.A. Sadough is with the Department of Mechanical Engineering, Amirkabir University of Technology, Tehran, Iran (E-mail: sadough@aut.ac.ir)
iv M. Saffar Avval is with the Department of Mechanical Engineering, Amirkabir University of Technology, Tehran, Iran (E-mail: mavval@aut.ac.ir)

A methodology is presented to determine numerically the heat transfer coefficients and the film thickness between the plates. The channel can be either two vertical parallel plates or cylinder. The saturated steam will be condensed in the channel because of the wall temperature (T_w), is lower than the saturation temperature of steam. It should be noted that the average steam velocity is not constant along *x*-direction. Since condensation occurs on the wall, the amount of steam flow in the core is reduced.

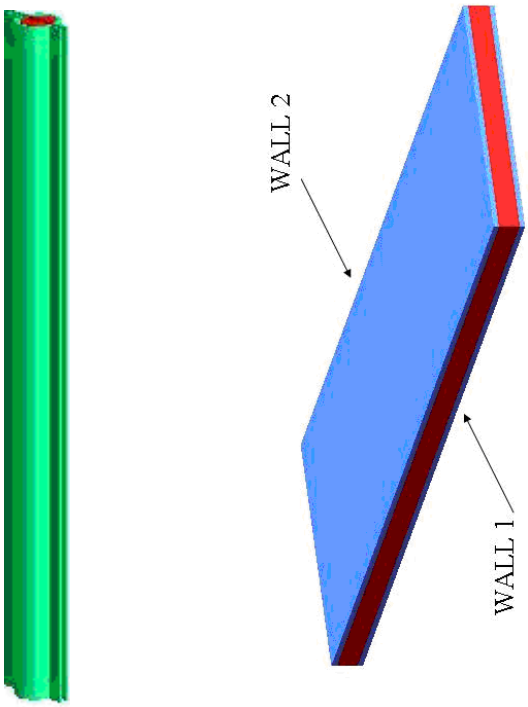

Fig.1. Geometrical model of vertical parallel plates and cylinder.

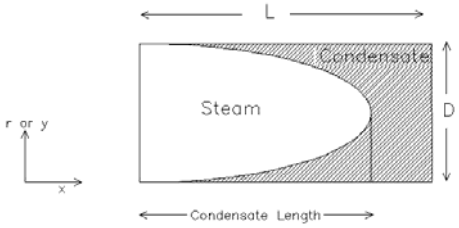

Fig.2. Physical model of the vertical parallel plates or cylinder.

The following assumptions have been made in order to solve the condensation flow:

1- Vapor and liquid phases are both incompressible and, therefore the density for each phase is constant.
2- Steam is saturated, therefore there is no saturated temperature gradient
3- The working fluid along the liquid-vapor phase is saturated.

In order to simplify the solution procedure, one set of governing equations for both the liquid and vapor regions are as follows:

Continuity Equation for each phase:

$$\frac{\partial}{\partial t}\left(\alpha_q \rho_q\right)+\nabla.(\alpha_q \rho_q \vec{V}_q)=0.0 \quad (1)$$

VOF Equation:

$$\frac{\partial \alpha_q}{\partial t}+\vec{V}.\nabla \alpha_q=\frac{S_{\alpha q}}{\rho_q} \quad (2)$$

$S_{\alpha q}$ is the source term for condensation or evaporation. *q* is the secondary phase index and it should be noted that, it is not necessary to calculate secondary phase independently because of the relation between primary and secondary phases which is as follows:

$$\sum_{p=1}^{n}\alpha_P=1 \quad (3)$$

$$\alpha_p=1-\alpha_q \quad (4)$$

The continuity equation for a cell consists of the gas-liquid interface will be obtained as follows:

$$\frac{\partial}{\partial t}(\rho_l\alpha_l)+\frac{\partial}{\partial t}(\rho_g\alpha_g)+\nabla.\left(\alpha_l\rho_l\vec{V}_l\right)+\nabla.\left(\alpha_g\rho_g\vec{V}_g\right)=0 \quad (5)$$

$$S_{m_{g-l}}=-[\frac{\partial}{\partial t}(\rho_g\alpha_g)+\nabla.\left(\alpha_g\rho_g\vec{V}_g\right)] \quad (6)$$

$$S_{m_{l-g}}=-S_{m_{g-l}}=-[\frac{\partial}{\partial t}(\rho_l\alpha_l)+\nabla.\left(\alpha_l\rho_l\vec{V}_l\right)] \quad (7)$$

The right hand side of equation (11) is written as follows:

$$\frac{\partial}{\partial t}(\rho_l\alpha_l)+\nabla.\left(\alpha_l\rho_l\vec{V}\right)=\frac{\partial}{\partial t}(\rho_l\alpha_l)+\vec{V}.\nabla(\alpha_l\rho_l)+\alpha_l\rho_l\nabla.\vec{V}= \quad (8)$$

$S_{m_{g-l}}$

So, *VOF* equation for liquid phase as secondary phase is obtained as follows:

$$\rho_l\frac{D\alpha_l}{Dt}=S_{m_{g-l}}-\alpha_l\rho_l\nabla.\vec{V} \quad (9)$$

$$\frac{D\alpha_l}{Dt}=\frac{S_{m_{g-l}}}{\rho_l}-\alpha_l\nabla.\vec{V} \quad (10)$$

$S_{m_{g-l}}$ is the mass source term and can be defined by $\dot{m}'''$.

So, *VOF* equation for primary and secondary phases is:

$$\frac{D\alpha_l}{Dt}=\frac{\dot{m}'''}{\rho_l}-\alpha_l\nabla.\vec{V} \quad (11)$$

$$\frac{D\alpha_v}{Dt}=\frac{\dot{m}'''}{\rho_v}-\alpha_v\nabla.\vec{V} \quad (12)$$

Summation of the above equations is as follows:

$$\frac{D\alpha_v}{Dt}+\frac{D\alpha_l}{Dt}=\dot{m}'''(\frac{1}{\rho_l}-\frac{1}{\rho_v})-\nabla.\vec{V} \quad (13)$$

$$\frac{D\alpha_v}{Dt}+\frac{D\alpha_l}{Dt}=\frac{D(1)}{Dt}=0.0 \quad (14)$$

So,

$$\nabla.\vec{V}=\dot{m}'''[\frac{1}{\rho_l}-\frac{1}{\rho_v}] \quad (15)$$

Finally, *VOF* equation for liquid phase is obtained:

$$\frac{D\alpha_l}{Dt}=\frac{\dot{m}'''}{\rho_l}-\alpha_l\dot{m}'''[\frac{1}{\rho_l}-\frac{1}{\rho_v}] \quad (16)$$

ρ_l, ρ_g are the liquid and gas densities and α_l is the volume fraction of the liquid phase.

Energy equation for condensation without radiation term is:

$$\frac{\partial}{\partial t}(\rho H)+\nabla.(\vec{V}(\rho H+P))=\nabla.(K_{eff}\nabla T) \quad (17)$$

$$H=h+\Delta H \quad (18)$$

where h and ΔH represent contributions of sensible enthalpy and latent heat on the total enthalpy, i.e., so it can be rearranged the equations as follows:

$$\frac{\partial}{\partial t}(\rho h)+\frac{\partial}{\partial t}(\rho\Delta H)+\nabla.(\vec{V}(\rho h+P))+\nabla.(\vec{V}(\rho\Delta H))=\nabla.(K_{eff}\nabla T) \quad (19)$$

$$\frac{\partial}{\partial t}(\rho h)+\nabla.(\vec{V}(\rho h+P))=$$

$$\nabla.(K_{eff}\nabla T)-[\frac{\partial}{\partial t}(\rho\Delta H)+\nabla.(\vec{V}(\rho\Delta H))] \quad (20)$$

So, energy source term can be defined as follows,

$$S_{\Delta H}=-[\frac{\partial}{\partial t}(\rho\Delta H)+\nabla.(\vec{V}(\rho\Delta H))] \quad (21)$$

The Total Enthalpy can be defined as follows:

$$H=\frac{\rho_v\alpha_v(H_v)+\rho_l\alpha_l(H_l)}{\rho}=\frac{\rho\alpha_v(h_v+h_{fg})+\rho_l\alpha_l h_l}{\rho} \quad (22)$$

As $H_l=h_l$ so,

$$H=\frac{\rho_v\alpha_v h_v+\rho_v\alpha_v h_{fg}+\rho_l\alpha_l h_l}{\rho} \quad (23)$$

$$H=h+\frac{\rho_v\alpha_v h_{fg}}{\rho} \quad (24)$$

$$\Delta H=\frac{\rho_v\alpha_v h_{fg}}{\rho} \quad (25)$$

$$S_{\Delta H}=-[\frac{\partial}{\partial t}(\frac{\rho\,\rho_v\alpha_v h_{fg}}{\rho})+\nabla.(\vec{V}(\frac{\rho\,\rho_v\alpha_v h_{fg}}{\rho}))] \quad (26)$$

$$S_{\Delta H}=-\rho_v h_{fg}[\frac{\partial}{\partial t}(\alpha_v)+\nabla.(\vec{V}\alpha_v)] \quad (27)$$

The relation between mass and energy source term is defined by below equation:

$$\frac{S_{\Delta H}}{h_{fg}}=\dot{m}''' \quad (28)$$

3. NUMERICAL SOLUTION

The Overall numerical solution procedure for a particular time step is outlined as follows:

Step1. *VOF* equation has to be solved.

Step2. Momentum and Continuity equations should be solved.

Step3. In generals, energy equation should be solved except the interface regions.

Convective term in energy equation can be legally omitted on gas-liquid interface because the velocity of the liquid phase is suddenly decreased regarding condensation phenomena. So, a linear approximation can be used to calculate energy source term as follows:

$$S_{\Delta H}=(K\frac{dT}{dr}A)_{gas}-(K\frac{dT}{dr}A)_{liq} \quad (29)$$

The first term of right hand side of equation (29) is zero, because there is no gradient in temperature for gas phase and therefore the energy source term should be identified as follow:

$$S_{\Delta H}=K_{liq}A_{wall}\frac{(T_{sat}-T_{wall})}{y_{cell}-y_{wall}} \quad (30)$$

It is obvious that, for control volumes that exist on liquid-gas interface, the amount of temperature is exactly saturated temperature of the steam. So, for control volumes including the interface, the temperature are set to the saturation temperatures by a user define functions that should be added to the software.

Step4. Equation (28) is used to determine the mass production rate.

Step5. Compute the source term for the VOF equation and the continuity equation.

Step6. Going back to step1 until the residuals for pressure, momentum and enthalpy meet the acceptable range (below than 0.001).

It should be noted that, these steps are all doing for each time step. After the solution for the current time step is obtained, the computation for the next time step is performed. These steps are added to Fluent software by a *C*++ code. As is shown in Fig. 3, User Define Function is written in order to define mass and energy source term according to the mentioned algorithm.

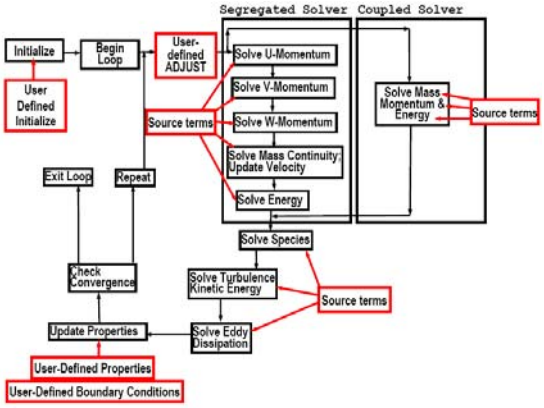

Fig. 3. Solvers Flowchart in Fluent.

4. RESULTS AND DISCUSSION

4.1. Verifications

A verification of the numerical method was performed by analytical simulating the condensation in a condenser section of a thermosyphone worked by Seban and Faghri[18]. The geometric configuration of the problem is a cylindrical tube as the same as present work, except that the tube is closed at x=0 and the effect of gravity must be taken into account. The tube is vertical, and the gravity acts in the x-direction. Vapor is injected to the tube and moved under effect of the gravity. The complete geometry is defined in Ref. [18]. The radius and the length of the circular tube are R=1.2 mm and L=4.0 cm, respectively. The working wall temperature is 310.8 K. The comparison between the numerical result of Seban and Faghri and present work is shown in Table (1).

Verification has been done by comparison between present numerical simulation and experimental investigations done by Wurfel et al. [12]. In their experimental work, they obtained a correlation for condensation flow between herringbone-type parallel plates in plate type heat exchangers. [12]

The comparison between experimental results of Wurfel et. al. [12] and present work is shown in Table (1) as well. As it is shown in Table (1), herringbone-type chevrons causes an increase in the Nusselt number in comparison with cylindrical chevron investigated in the present research.

To verify numerical simulation of condensation heat transfer coefficient, numerical results were compared with results obtained by Kafi et al. [19]. They provided an experimental set up to simulate two-phase flow phenomena between the plates in a single effect thermal desalination unit. Their system was under vacuum and saturated steam temperature in their experimental set up was 70^{o}C. The comparison between results of Kafi et al. and present work is shown in Table (1) as well.

Table 1. Comparison of the average Nusselt Number of present results and others in similar case.

	Others Result	Present Work
Seban and Faghri	38.4	39.6
Wurfel et al.	95	38
Kafi et al.	32	38

At last, final verification in laminar condensation between parallel plates has been done by comparison between the numerical results of Zhang and Faghri [20] and the present work in similar case. The geometric configuration of Zhang and Faghri's model is a horizontal miniature channel. Saturation temperature in their model is 363 K and wall temperature is 340 K. Inlet velocity of the vapor is 0.2 m/s. Fig. 4a and Fig. 4b show heat transfer coefficients obtained by Zhang and Faghri[20] in comparison with the present work. As they assumed a small thickness of condensation boundary layer to avoid divergence problem at the beginning of the plates as a single point with maximum mass and energy source term, there is a difference in their results in comparison with present results at the beginning of condensation.

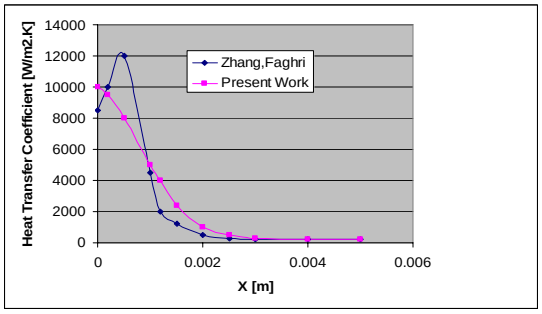

Fig. 4a. Comparison of heat transfer coefficient between parallel plates.

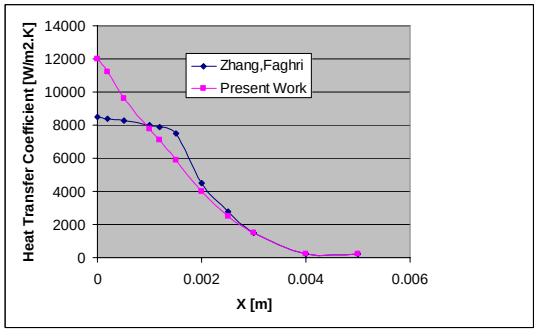

Fig. 4b. Comparison of heat transfer coefficient in circular tube.

Finally, the overall agreement can be seen between the present result and the previous work.

4.2. Condensation between parallel plates

Condensation phenomena formed by two vertical parallel plates is investigated in this section. The gap between the plates and the length of the channel are

assumed: D=4mm and L=0.2 m respectively. The effect of the gravity is considered in X direction and neglected in Y direction. A non uniform grid of 100(x)*50(y) with a time step of $\Delta t = 10^{-5}$ was used. Fig. 4 and Fig. 5 show the contour of volume fraction of laminar and turbulent condensation flow along the vertical parallel plates. Inlet velocity of vapor flow in laminar flow is 1 m/s and 20 m/s for turbulent flow. Condensation flow is fully developed at the end of the plates. A wavy regime is completely visible in turbulent condensation flow between the parallel plates.

Contour of velocity vectors for laminar condensation flow and streamlines for turbulent condensation flow are shown in Fig. 5a and Fig. 5b. As seen, the mass flow rate is constant and the density of the liquid is much greater than the vapor, so since condensation occurs near the wall on vapor-liquid interface, the vapor velocity vectors near the wall point towards the wall and the mean vapor velocity decreases with x, due to condensation. In case of turbulent condensation flow regarding high velocity at inlet flow and high amount of surface tension between vapor and liquid phase, some vortex flow can be created along the flow between the plates near the wall and near the vapor-liquid interface.

Fig.5a. Contour of volume fraction of laminar condensation flow between vertical parallel plates.

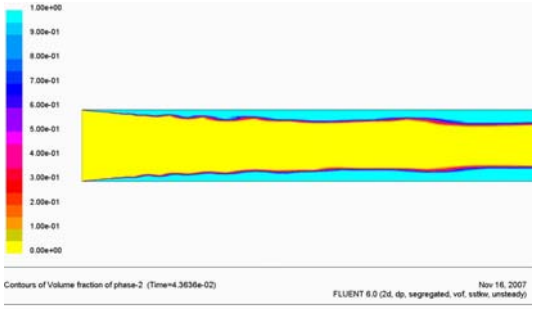

Fig.5b. Contour of volume fraction of turbulent condensation flow between vertical parallel plates.

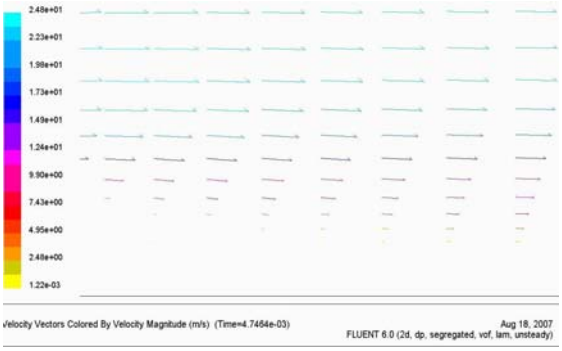

Fig.6. Contour of velocity vectors of laminar condensation flow between parallel vertical plates.

Heat transfer coefficient, of laminar and turbulent condensation flow between parallel plates is shown in Fig. 8 and Fig. 9. As shown, the amount of heat transfer coefficient is decreased after capillary blocking because the amount of heat transfer coefficient directly depends on boundary layer thickness. In turbulent flow case capillary blocking is occurred faster but because of high inlet velocity and high amount of Reynolds number. Average heat transfer coefficient in turbulent case is much greater than laminar case. In addition, there is some oscillation in heat transfer coefficient curve regarding the vortex flows that can be observed in turbulent cases.

Fig.7. Streamlines of turbulent condensation flow between vertical parallel plates.

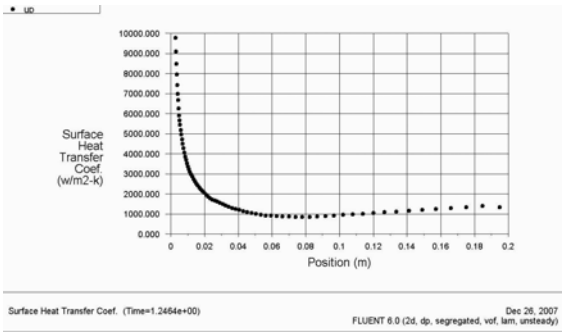

Fig.8. Heat transfer coefficient of laminar condensation flow between vertical parallel plates.

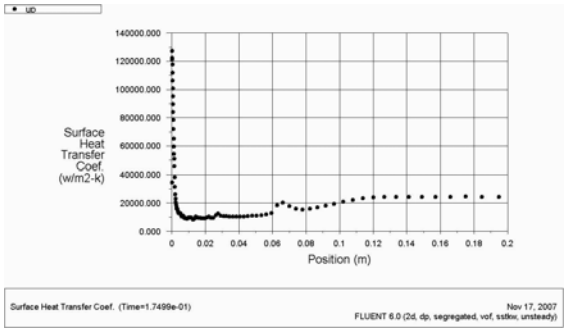

Fig.9. Heat transfer coefficient of turbulent condensation flow between vertical parallel plates.

The effect of variation in Reynolds number of inlet steam between the plates on condensation heat transfer coefficient is shown in Fig. 10. As shown in this figure, by increasing the Reynolds Number of inlet steam between the plates, the amount of heat transfer coefficient will increase but the rate of the increase in heat transfer coefficient at lower Reynolds number is more than higher Reynolds number.

The effect of distance between parallel plates on condensation is shown in Fig.11. The mass flow rates of inlet steam in all cases are the same and so by the decrease in the distance between the plates the amount of velocity and Reynolds number will increase. Therefore, the amount of heat transfer coefficient will increase.

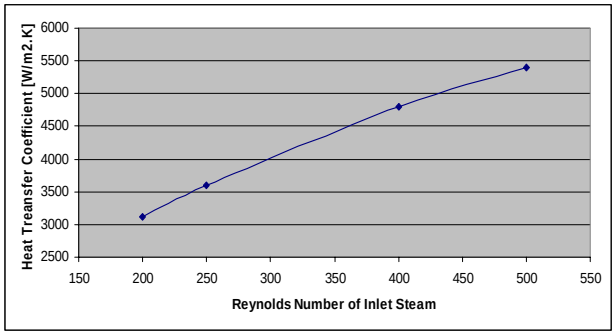

Fig.10. Effect of Reynolds number of inlet steam on heat transfer coefficient

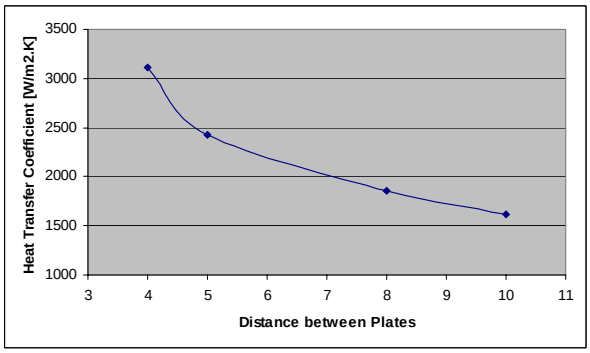

Fig.11. Effect of distance between vertical parallel plates on heat transfer coefficient.

The effect of inlet velocity on heat transfer coefficient in laminar condensation flow is shown in Fig 12. By increasing the inlet velocity between the parallel plates the Reynolds number will increase and the rate of increasing the boundary layer thickness will decrease so the amount of heat transfer coefficient will increase as a result.

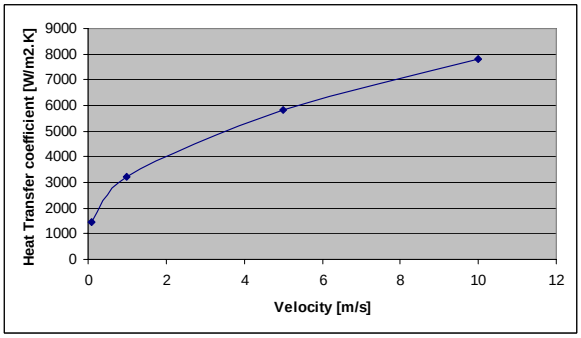

Fig.12. Effect of inlet velocity on heat transfer coefficient.

In Fig. 13, it is seen that the amount of heat transfer coefficient will increase by the decrease in the temperature difference between the wall and the saturation temperature of steam because condensation rate will increase by increasing the amount of temperature difference so capillary blocking will move to the beginning of the plates therefore the average of heat transfer coefficient will decrease under effect of a fully developed condensation between the plates.

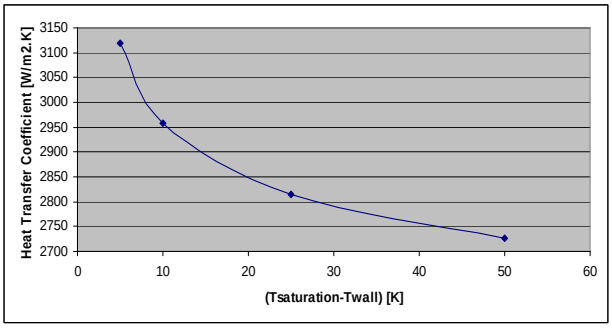

Fig.13. The effect of temperature difference between the wall and the saturation temperature on heat transfer coefficient.

4.3. Condensation in cylindrical chevron

When two vertical parallel plates with semi cylindrical vertical chevron are assembled with a gasket between them, a cylindrical vertical tube is formed as shown in Fig. 14. Also, if the wall temperature is lower than the saturation temperature, steam flow is condensed in this cylindrical vertical chevron.

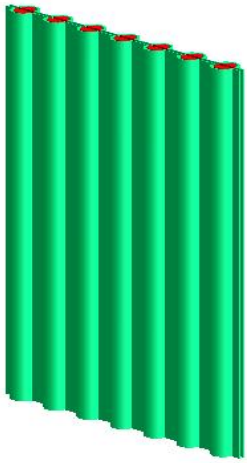

Fig.14. Cylindrical vertical tube formed by two vertical parallel plates.

Condensation phenomena formed by vertical cylindrical chevron are investigated as well. The diameter of the chevrons between the plates and the length of the channel are: D=4mm and L=0.2 m. The effect of gravity is considered in direction of X axis and is neglected in Y axis, therefore this is an axisymmetric problem so only half of the domain ($0<y<D/2$) is solved. A non uniform grid of $100(x)*50(y)$ with a time step of $\Delta t = 10^{-5}$ is used to solve this problem.

Fig. 15 and Fig. 16 show the contour of volume fraction of laminar and turbulent condensation flow along the vertical cylindrical chevron. Inlet velocity of vapor flow in laminar flow is 1 m/s and 20 m/s for turbulent flow. In laminar case, condensate flow is fully developed after about 4 cm from the entrance.

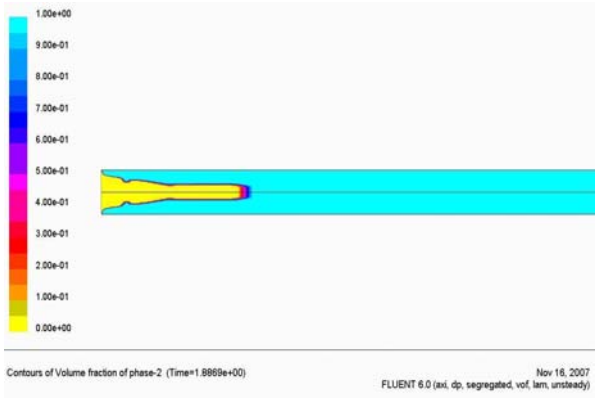

Fig.15. Contour of volume fraction of laminar condensation flow inside the vertical cylindrical chevron.

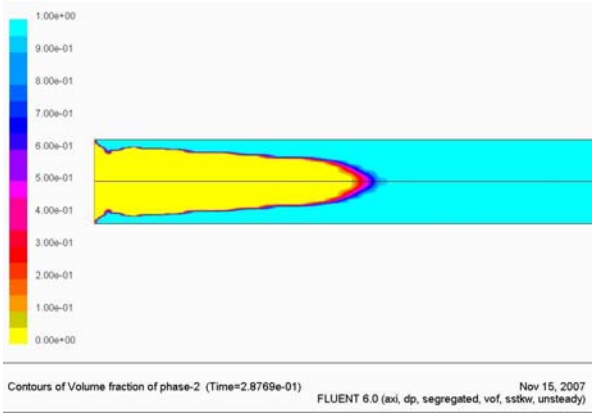

Fig.16. Contour of volume fraction of turbulent condensation flow inside the vertical cylindrical chevron.

Boundary layer is wavy shape in turbulent case and fully developed condensation flow can be observed after approximately 8 cm from the entrance.

Contour of velocity vectors for laminar condensation flow and streamlines for turbulent condensation flow are shown in Fig. 17 and Fig. 18. As the same as the previous case in parallel plates, the mass flow rates are constant and the density of the liquid is greater than the vapor. So, since the condensation occurs on the wall, the vapor velocity vectors near the wall point and vapor-liquid interface towards the wall and the mean vapor velocity decreases with x, due to the condensation. In case of turbulent condensation flow regarding high velocity at inlet flow and surface tension between the phases, some vortex flow can be created near the wall as the same as flow between parallel plates.

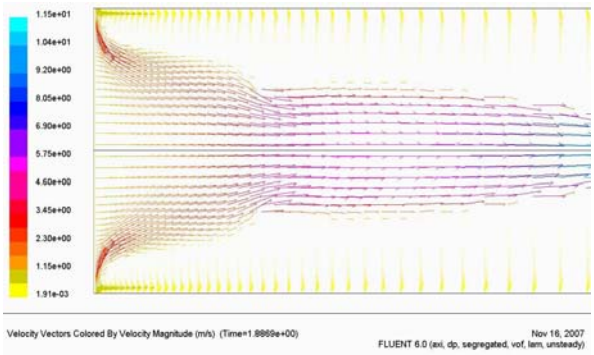

Fig.17. Contour of velocity vectors of laminar condensation flow inside the cylindrical chevron.

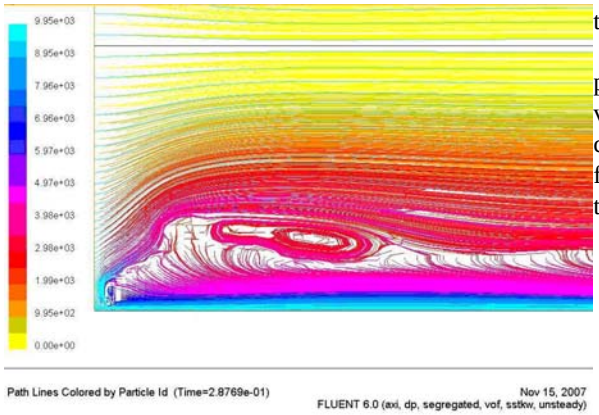

Fig.18. Streamlines of turbulent condensation flow inside the cylindrical chevron.

Variation of the heat transfer coefficient of laminar and turbulent condensation flow in vertical cylindrical chevron is shown in Fig. 19 and Fig. 20. As shown in Fig. 19, in spite of the high amount of heat transfer coefficient in inlet flow, the amount of heat transfer coefficient is decreased rapidly after capillary blocking. It can be seen that fully developed condensation is occurred along the first half of the cylinder and amount of heat transfer coefficient is constant and same as a single phase liquid flow inside vertical circular tubes after steam condensation.

In turbulent flow case in Fig. 20, because of high inlet velocity, average heat transfer coefficient is much greater than laminar case. It can be seen that the amount of heat transfer coefficient has a different trend in turbulent flow in comparison with laminar flow case because of the effect of vortex flow along the cylindrical chevron. Also, it can be seen that there are some oscillations in heat transfer coefficient curve under the effect of entrance region especially in turbulent case.

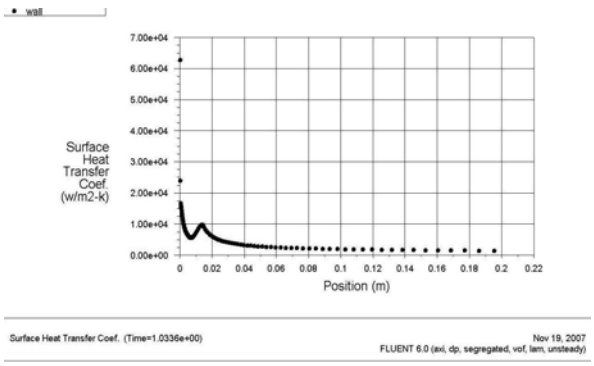

Fig.19. Heat transfer coefficient of laminar condensation flow inside the vertical cylindrical chevron.

Optimum length for cylindrical chevron between the plates for a constant diameter is the length that the fully developed condensation occurs exactly at the end of the plates. The amount of heat transfer coefficient will meet the maximum value in this case.

Effect of cylindrical chevron diameter between parallel plates on condensation is shown in Fig.21. The inlet velocity in all cases is same and so by the increase in the cylindrical chevron diameter between the plates, the mass flow rate and Reynolds number will increase. As a result, the amount of heat transfer coefficient will increase.

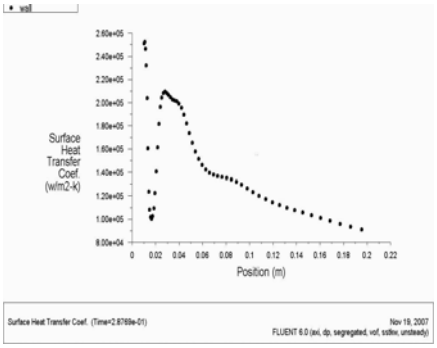

Fig.20. Heat transfer coefficient of turbulent condensation flow inside the vertical cylindrical chevron.

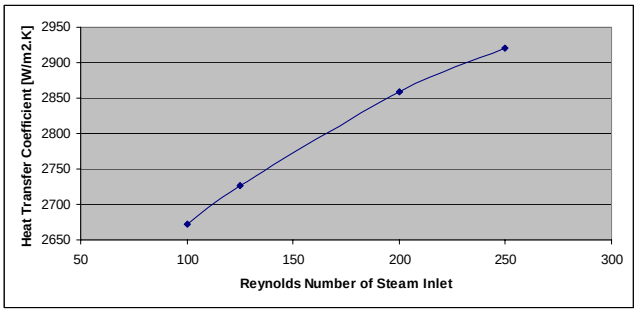

Fig.21. Effect of variation in Reynolds number on heat transfer coefficient in cylindrical chevron.

The effect of cylindrical chevron diameter between parallel plates on condensation is shown in Fig.22. The mass flow rate of inlet steam in all cases is same and so by decreasing the chevron diameter between the plates, the Reynolds number will increase so the amount of heat transfer coefficient will increase, respectively. The optimum diameter for cylindrical chevrons with a constant length is the case that the fully developed condensation occurs at the end of the plates.

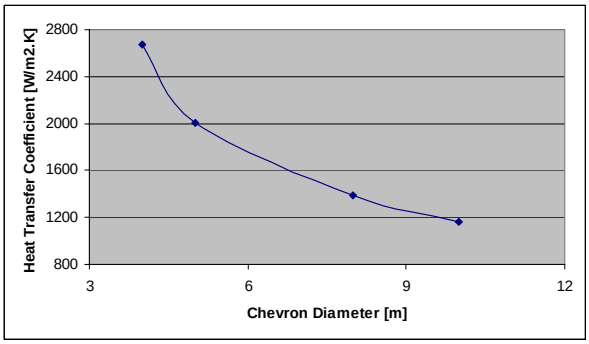

Fig.22. Effect of chevron diameter on heat transfer coefficient.

Effect of inlet velocity on heat transfer coefficient in laminar condensation flow is investigated in Fig 23 for cylindrical chevron. By the increase in the inlet velocity, the Reynolds number will increase so the amount of heat transfer coefficient will increase, respectively. At higher velocity, under the effect of high amount of velocity and wavy shape of boundary layers, it can be seen that the amount of heat transfer coefficient will increase rapidly in comparison with lower velocities.

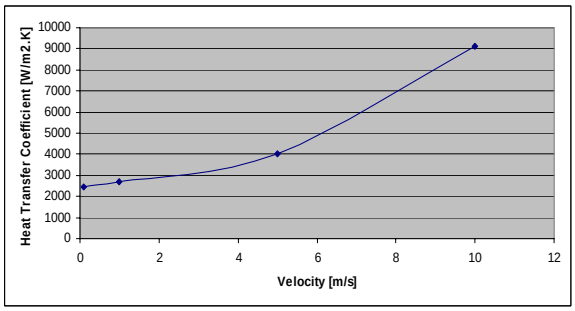

Fig.23. Effect of inlet velocity in cylindrical chevron on heat transfer coefficient.

In Fig. 24, it is seen that as the same as the flow between parallel plates the amount of heat transfer coefficient will increase by decreasing the temperature difference between the wall and the saturation temperature in vertical cylindrical chevron. The rate of condensation will increase by increasing the temperature difference between saturation temperature and wall temperature therefore fully developed condensation flow is occurred inside the cylindrical chevron and so the average heat transfer coefficient will decreased along the cylinder.

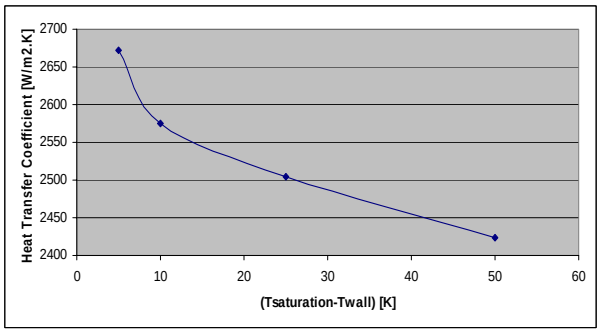

Fig.24. Effect of temperature difference between the wall and the saturation temperature on heat transfer coefficient in cylindrical chevron.

The amount of heat transfer coefficient in all cases is strongly depending on the boundary layer thickness. Steam velocity and temperature difference between the wall and saturation temperature has an effect on boundary layer thickness. The rate of increasing boundary layer thickness will increase by decreasing the inlet velocity or increasing in chevron diameter or distance between the plates. Therefore, in chevrons with higher diameter, in spite of higher distance between the walls, since the velocity is low, the rate of increasing in boundary layer thickness will increase and so the amount of heat transfer will decrease.

One of the most interesting subjects in condensation phenomena is the difference between the front of single phase flow and phase change flow. The difference between single phase flow front and phase change front is shown in Fig. 25. The comparison between single phase front and phase change front shows that the rate of the increase in boundary layer thickness in single phase flows is more than for phase change. In addition, a flat and vertical surface can be seen at the end of the phase change flow front but in single phase case boundary layer is similar to a parabolic shape.

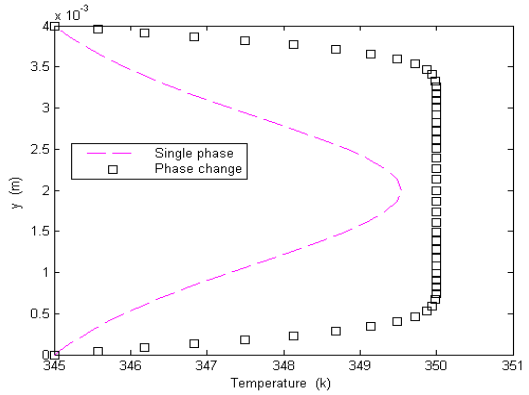

Fig. 25. Comparison between phase change and single phase flow front.

5. CONCLUSIONS

Numerical simulation for condensation in vertical parallel plates and vertical cylindrical chevron is performed using VOF method. The effect of various physical and geometric parameters on heat transfer coefficient for both vertical parallel plates and vertical cylindrical chevron are investigated. The results show that the condensation heat transfer coefficient increases sharply by the increase in the inlet velocity and the decrease in the temperature difference between the wall and saturation temperature of inlet steam. By parametric study, it can be concluded that in order to reach the maximum heat transfer coefficient in plate type heat exchangers, the number of plates should be minimized with consideration of allowable pressure drop. Velocity vectors in all cases are toward the wall. The wavy shape of liquid film and some vortex flow were observed for the cases with high vapor velocity in turbulent flows. There are noticeable changes between single phase boundary layer and phase change boundary layer. Maximum value for heat transfer coefficient will be obtained if the fully developed condensation occurs exactly at the end of the plates. Result shows that maximum heat transfer

coefficient will be achieved if the distance between the plates is 4mm and the length of the plates is 20 cm.

6. ACKNOWLEDGMENT

Authors would like to express their appreciation to the Fan-Niroo Company (Tehran, IRAN), for their valuable cooperation and also thanks to Bonian-Daneshpajouhan Institute (Tehran, IRAN) and our co-workers particularly Mr. Asgari and Mr. Asghari.

7. REFERENCES

[1] Kakac, S., A.E. Bergles, F. Mayinger, "Heat Exchanger,Thermal-Hydraulic Fundamentals and Design", Hemisphere publication, Mc Graw-Hill Book Company 198.

[2] Saunders, E. A.D., "Heat Exchangers", John Wiley & Sons, Inc, 1988.

[3] W.X. Jin, S.C. Low, Terence Quek, "Preliminary experimental study of falling film heat transfer on a vertical doubly fluted plate", Journal of Desalination 152 (2002) 201-206.

[4] C.P. Ribeiro Jr., M.H. Andrade, "A heat transfer model for the steady-state simulation of climbing-falling-film plate evaporators", Journal of Food engineering 54 (2002) 309-320.

[5] M. El Haj Assad, Markku J. Lampinen, "Mathematical modeling of falling liquid film evaporation process", International Journal of Refrigeration 25 (2002) 985-991.

[6] S. Wellsandt, L. Vamling, "Heat transfer and pressure drop in a plate-type evaporator", International Journal of Refrigeration 26 (2003) 180-188.

[7] Lieke Wang, Bengt Sunden, "Optimal design of plate heat exchangers with and without pressure drop specifications", Applied Thermal Engineering 23 (2003) 295-311.

[8] Jorge A. W. Gut. Jose M. Pinto, "Modeling of plate heat exchangers with generalized configurations", International Journal Heat and Mass Transfer 46 (2003) 2571-2585.

[9] Dong-Hyouck Han, Kyu-Jung Lee, Yoon-Ho Kim, "Experiments on the characteristics of evaporation of R410A in brazed plate heat exchangers with different geometric configurations", Applied Thermal Engineering 23 (2003) 1209-1225.

[10] Yoichi Shiomi, Shigeyasu Nakanishi, Takafumi Uehara, "Characteristics of two-phase flow in a channel formed by chevron type plates", Experimental Thermal and Fluid Science 28 (2004) 231-235.

[11] Jorge A. W. Gut, Jose M. Pinto, "Optimal configuration design for plate heat exchangers", International Journal Heat and Mass Transfer 47 (2004) 4833-4848.

[12] Reinhard Wurfel, Nikolai Ostrowski, "Experimental investigations of heat exchangers of the herringbone-type" ,International Journal of thermal sciences 43 (2004) 59-68.

[13] P. K. Pandy, "Two-dimensional turbulent film condensation of vapors flowing inside a vertical tube and between parallel plates: a numerical approach", Refrigeration J., 26 (2003) 492-503.

[14] G.A. Longo , A. Gasparella, R. Sartori, "Experimental heat transfer coefficients during refrigerant vaporisation and condensation inside herringbone-type plate heat exchangers with enhanced surfaces", International Journal Heat and Mass Transfer 47 (2004) 4125-4136.

[15] Henning Raach, Jovan Mitrovic, "Simulation of heat and mass transfer in a multi effect distillation plant for seawater desalination", Journal of Desalination 183 (2005) 307-316

[16] R.K.Kamali, A. Abbassi, S.A. Sadough, "A simulation model and parametric study of MED-TVC process", EDS international conference, EuroMed (2006) 118-123.

[17] KouhiKamali R., Abbassi, A., Sadough, S. A., Saffar Avval, M., "Thermodynamic Design and Parametric study of MED-TVC", Desalination J., 222(2008) 607-615.

[18] Seban, R. A., and Faghri, A., 1984, "Film Condensation in a Vertical Tube with a Closed Top", Int. J. Heat Mass Transfer, pp. 944-948.

[19] F. Kafi, V. Renaudin, D. Alonso, J.M. Hornut, "New MED plate desalination process: Thermal performances", Journal of Desalination 166 (2004) 53-62.

[20] Zhang, Y., Faghri, A., Shafii, M. B., 2001, "Capillary Blocking in Forced Convective condensation in Horizental Miniature Channels", Journal of Heat Transfer, pp. 501-510.